Atmos. Chem. Phys. Discuss., https://doi.org/10.5194/acp-2019-397
Manuscript under review for journal Atmos. Chem. Phys.
Discussion started: 6 May 2019

Atmospheric Chemistry and Physics Discussions
Open Access

A revisit of parametrization of summer downward longwave radiation over the Tibetan Plateau from high temporal resolution measurements

Mengqi Liu[a,c], Xiangdong Zheng[d*], Jinqiang Zhang[a,b,c] and Xiangao Xia[a,b,c*]

[a] LAGEO, Institute of Atmospheric Physics, Chinese Academy of Sciences, Beijing, 100029, China

[b] Collaborative Innovation Center on Forecast and Evaluation of Meteorological Disasters, Nanjing University of Information Science & Technology, Nanjing 210044, China

[c] College of Earth and Planetary Sciences, University of Chinese Academy of Sciences, Beijing, 100049, China

[d] Chinese Academy of Meteorological Sciences, Beijing, 100081, China

Corresponding author:

Dr. Xiangdong Zheng

Chinese Academy of Meteorological Sciences, Beijing, 100081, China

Email: xdzheng@cma.gov.cn

Phone: 86-10-58995272

Dr. Xiangao Xia

LAGEO, Institute of Atmospheric Physics, Chinese Academy of Sciences, China

Email: xxa@mail.iap.ac.cn

Phone: 86-10-82995071

Abstract

The Tibetan Plateau (TP) is one of hot spots in the climate research due to its unique geographical location, high altitude, highly sensitive to climate change as well potential effects on climate in East Asia. Downward longwave radiation (DLR), as a key component in the surface energy budget, is of practical implications for many research fields. Several attempts have been made to measure hourly or daily DLR and then model it over the TP. This study uses 1-minute radiation and meteorological measurements at three stations over the TP to parameterize DLR during summer months. Three independent methods are used to discriminate clear-sky observations by making maximal use of collocated measurements of downward shortwave and longwave radiation as well as Lidar backscatter measurements with high temporal resolution. This guarantees a reliable separation of clear-sky and cloudy samples that favors for proper parameterizations of DLR under these two contrast conditions. Clear-sky and cloudy DLR models with original parameters are firstly assessed. These models are then locally calibrated based on 1-minute observations. DLR estimation is notably improved since specific conditions over the TP are accounted for by local calibration, which is indicated by smaller root mean square error (RMSE) and larger coefficient of determination (R^2). The best local parametrization can estimate clear-sky DLR with RMSE of 3.8 $W \cdot m^{-2}$. Overestimation of clear-sky DLR by previous study is evident, likely due to potential residue cloud contamination on the clear-sky samples. Cloud base height under overcast conditions is shown to be intimately related to cloudy DLR parameterization, which is considered by this study in the locally calibrated parameterization over the TP for the first time.

Atmos. Chem. Phys. Discuss., https://doi.org/10.5194/acp-2019-397
Manuscript under review for journal Atmos. Chem. Phys.
Discussion started: 6 May 2019

1 Introduction

Downward longwave radiation (DLR) at the Earth's surface is the largest component of the surface energy budget, being nearly double downward shortwave radiation (DSR) (Kiehl and Trenberth, 1997). DLR has shown a remarkable increase during the process of global warming (Stephens et al., 2012). This is closely related to the fact that both a warming and moistening of the atmosphere (especially at the lower atmosphere associated with the water vapor feedback) positively contribute to this change. Understanding of complex spatiotemporal variation of DLR and its implication is essential for improving weather prediction, climate simulation as well as water cycling modeling. Unfortunately, uncertainties in DLR are considered substantially larger than that in any of the other components of surface energy balance, which is most likely related to scarce DLR measurements with high quality (Stephens et al., 2012).

The 2-sigma uncertainty of DLR measurement by using a well-calibrated and maintained pyrgeometer is estimated to be 2.5% or 4 W m^{-2} (Stoffel, 2005). However, the global-wide surface observations are very limited, especially in those remote regions. DLR is extensively estimated by proxy meteorological measurements of synoptic variables. It has been known for almost one century that the clear-sky DLR is determined by the bulk emissivity and effective temperature of the overlying atmosphere (Angstrom, 1918). Since these two quantities are not easily observed for a vertical column of the atmosphere, clear-sky DLR is alternatively parameterized as a function of air temperature and water vapor density, assuming that the clear sky radiates toward the surface like a grey body at a screen-level temperature (the standard level of meteorological measurements, generally 1.5 m above the ground). Dozens clear-sky DLR models have been developed by parameterization of different clear-sky effective emissivity (ε_c) to the screen-level temperature (T_a) and water vapor pressure (e). Exponential function (Idso, 1981) or power law function (Brunt, 1932) have been widely used to depict the relationship of ε_c to T_a and/or e. The coefficients of these functions are generally derived by a regression analysis of collocated measurements of T_a, e and DLR. Most of these proposed parameterizations are thus empirical in nature and only specific for definite atmospheric conditions. Brutsaert (1975) was the first to develop a physically rigorous model of clear-sky atmospheric emissivity, which was based on the analytic solution of the Schwarzchild's equation for a standard atmospheric lapse rates of temperature and water vapor. Prata (1996) found that the precipitable water content (*w*) was much better to represent the effective emissivity of the atmosphere than *e*, which was loosely based on radiative transfer simulations. Dilley and O'Brien (1998) adopted this scheme but tuned empirically their parameterization using an accurate radiative transfer model. Given the fact that clear-sky DLR is impacted by water vapor and temperature profile (especially the inversion layer) and diurnal variation of T_a, a new model with two more coefficients considering these effects on DLR was developed (Dupont et al., 2008a).

In the presence of clouds, the total effective emissivity of the sky is remarkably modulated by clouds. The existing clear-sky parameterization should be modified according to the cloud fraction (CF) and other cloud parameters. CF is generally used to represent a fairly simple cloud modification under cloudy conditions. Many equations with cloudiness correction have been developed and evaluated by the DLR measurements across the world (Crawford and Duchon, 1999; Niemela et al., 2001). CF is widely obtained from surface human observations (Iziomon et al., 2003) that is subjective in nature. CF can also be derived from DSR (Crawford and Duchon, 1999) and/or DLR measurements (Durr and Philipona, 2004). Moreover, DSR or DLR measurements with very high temporal resolution (for example, 1-min) can also provide cloud type information (Duchon and Malley, 1999), and thereby allowing to consider the effects of cloud types on DLR (Orsini et al., 2002). This indicates that 1-min DSR and DLR measurements are beneficial to the DLR parameterization.

With an average altitude exceeding 4 km above the sea level (a.s.l.), Tibetan Plateau (TP), the largest mountain area in the world, exerts a huge influence on regional and global climate through mechanical and thermal forcings (Wu et al., 2007). TP is the region with very high sensitivity to climate change. The most rapid warming rate over the TP occurred in the latter half of the 20th century was likely associated with relatively large DLR increase. Duan and Wu (2006) indicated that increase in low level nocturnal cloud amount and thereby DLR can partly explain the increase in the minimum temperature, despite decreases in total cloud amount during the same period. By using observed sensitivity of DLR to change in specific humidity for the Alps, Rangwala et al. (2009) suggested that increase in water vapor appeared to be partly responsible for producing the large warming over the TP. Since the coefficients of these empirical models and their performances showed spatiotemporal variations, establishment of localized DLR parameterizations over the TP is of highly significance. Given the importance of DLR to climate change, further studies on the DLR parameterization as well as DLR sensitivity to atmospheric variables are desirable, which would expected to improve our understanding of climate change over the TP (Wang and Dickinson, 2013).

DLR measurements with high temporal resolution using high quality radiometer over the TP are quite scarce. So it is not surprising that there have been very few studies on DLR and its parameterization. Wang and Liang (2009) evaluated clear-sky DLR parameterizations of Brunt (1932) and Brutsaert (1975) at 36 globally distributed sites, in which DLR data at two TP stations were used. Yang et al. (2012) used hourly DLR data at 6 stations to study the major characteristics of DLR and the all-sky parameterization of Crawford and Duchon (1999) was assessed. More recently, Zhu et al. (2017) evaluated 13 clear-sky and 10 all-sky DLR models based on hourly DLR measurements at 5 automatic meteorological stations over the TP. Note that the CG3 pyrgemeters (Kipp & Zonen), the second class radiometer according to the International Organization for Standardization (ISO) classification, were used to measure DLR in these previous studies. The parameterization would thus be impacted by a large measurement uncertainty (roughly 10% according to the CG3 manual). Clear-sky and CF were determined with relative low temporal resolution, for example, subjectively by human observer every 3 or 6 hours, which would also impact the parameterization. One would expect that these previous methods developed for daily or longer-term averages were usually less accurate at shorter time intervals.

In order to further our understanding of DLR and DSR over the TP,

Atmos. Chem. Phys. Discuss., https://doi.org/10.5194/acp-2019-397
Manuscript under review for journal Atmos. Chem. Phys.
Discussion started: 6 May 2019

measurements of 1-min DSR and DLR at 3 stations over the TP using state-of-the-art instruments have been performed in summer months since 2011. These data provide us opportunity to evaluate clear-sky DLR models and quantitatively assess how cloud properties impact DLR. This study makes progress in the following aspects. Clear-sky discrimination and CF estimation are based on 1-min DSR and DLR measurements that are objective in nature. Misclassification of cloudiness into cloud-free skies would be minimized by adopting strict cloud-screening procedures based on not only 1-min DSR and DLR measurements but also coincident Lidar backscattering measurements. Potential effects of cloud-base height (CBH) on overcast DLR are investigated. Locally calibrated parameterizations of clear- and cloudy-sky DLRs are finally achieved.

2. Site, Instrument and Data

Measurements of DLR and DSR are conducted 1~4 months at three stations (Table 1), including Nagqu (NQ, 92.04°E, 31.29°N, 4.5 km a.s.l), Nyingchi(NC, 94.2°E, 29.4°N, 2.3 km a.s.l.) and Ali (AL, 80°E, 32.5°N, 4.3 km a.s.l.). DLR and DSR were measured by CG4 and CM21 radiometers, respectively. The sampling rate is 1 Hz and the averages of the samples over 1-min intervals are used. Simultaneous 1-min averages of T_a and e are taken from the automatic meteorological stations. CG4 is designed for the DLR measurement with high reliability and accuracy due to its specific material and unique construction. Window heating due to absorption of solar radiation in the window material is the major error source of DLR measurement, which is strongly suppressed by a unique construction conducting away the absorbed heat very effectively. The shading and un-shading experiment of CG4 measurements show a window heating offset of less than 4 $W \cdot m^{-2}$(Meloni et al., 2012), as a comparison, it can reach 25 $W \cdot m^{-2}$ for CG3 since it is always not shaded (Wang and Dickerson, 2013). An installation of the CG4 on the Kipp & Zonen CV2 ventilation unit is able to prevent dew deposition on the window. The radiometers are calibrated before and after field measurements through comparison to the reference radiometers operated by the national metrological standards of meteorology that is ultimately traceable to the World Infrared Standard Group.

A Micropulse Lidar (MPL-4B, Sigma Space Corporation, United States) was installed site-by-site with radiometers. The Nd:YLF laser of the MPL produces an output power of 12 μJ at 532 nm. The repletion rate is 2500 Hz. The vertical resolution of the MPL data is 30 m and the integration time of the measurements is 30 s. The MPL backscattering profiles are used to identify the cloud boundaries and derive the CBHs (He et al., 2013). The dataset contains about 700 hours of coincident DLR, DSR, Lidar and meteorological measurements.

3. Methods

3.1 Clear-sky discrimination

Clear skies should be discriminated from cloudy conditions before performing clear-sky DLR parametrization, which is achieved by the synthetical analysis of DSR, DLR, and CBH from MPL. The term clear sky or cloud-free in this paper means a sky without any condensed liquid or ice water for all classes of altitude.

Following the method initiated by Crwford and Duchon (1999), we calculate two quantities reflecting DSR magnitude and variability based on 1-min observed DSR (DSR_{obs}) and calculated clear-sky DSR (DSR_{cal}) values. DSR_{cal} is calculated by the model C of Iqbal (1983) in which direct and diffuse components of DSR on a horizontal surface are parametrized separately. Direct DSR is first calculated by multiplying transmittance due to Rayleigh scattering, aerosol attenuation and absorption by water vapor, ozone and the uniformly mixed gases. Diffuse DSR is estimated as the sum of the Rayleigh and aerosol scattering as well as the multiple reflected irradiance between surface and atmosphere. The terrain reflection is estimated according to Dozier and Frew (1990). The precipitable water is calculated from *e* according to a linear relationship that was developed based on collocated *e* and radiosonde (in AL) or GPS (NQ and NC) -based precipitable water measurements . Climatological value of aerosol optical depth and single scattering albedo are from the reference (Che et al., 2015). Mean surface albedo values of 0.22 at NQ, 0.18 at NC, and 0.25 at AL were from Liang et al. (2012).

1-min DSR_{cal} are first scaled to a constant value of 1400 $W \cdot m^{-2}$, which is used to normalize the DSR_{obs} by multiplying the same set of scale factors (Duchon and Malley, 1999; Long and Ackerman, 2000; Orsini et al., 2002). The mean and standard deviation of the scaled DSR_{obs} in a 21-min moving window (±10-min) centered on the time of interest are then calculated to discriminate clear-sky. Selection of the width of 21-min is empirical but a consequence of having a reasonable time span for estimating the mean and variance (Duchon and Malley, 1999). Clear-sky DSR should satisfy the followed three requirements: 1) ratio of DSR_{obs} to DSR_{cal} is within 0.95 to 1.05, 2) difference between scaled DSR_{obs} and DSR_{cal} is less than 20 $W \cdot m^{-2}$, and 3) standard deviation of scaled DSR_{obs} is less than 20 $W \cdot m^{-2}$. Temporal variability of DLR is also used to separate cloudy sky from cloud-free situations. Based on analysis of the standard deviation of scaled DLR (scaled to 500 $W \cdot m^{-2}$) for a ±10-min period, clear-sky periods are detected if the standard deviation is less than 5 $W \cdot m^{-2}$. Given the fact that DSR and DLR experience difficulties in detecting clouds in the portion of the sky far away from the sun (Duchon and Malley, 1999) or high-altitude cirrus clouds (Dupont et al., 2008b), coincident MPL backscatter measurements are used to strictly select clear-sky samples. We can be sure that there is a cloud element somewhere in the sky when the MPL identifies a cloud, we require that no clouds are detected by the MPL within the ±10-min period, otherwise it is defined as cloudy condition.

These two different methods are complementary to each other to some extent (Dupont et al., 2008b), one would expect that a combined analysis of both passive and active remote sensing instruments can precisely detect clear sky periods. We hence use the following strategy to select clear-sky samples. If DSR, DLR and MPL measurements at the time of interest synchronously satisfy specified clear-sky conditions, the sample is thought to be taken under unambiguously cloud-free condition; on the contrary, the measurement are made under unambiguously cloudy condition if all of these three methods suggests to be cloudy. Our following clear-sky and cloudy DLR parameterizations are respectively based on measurements under unambiguously cloud-free and cloudy conditions. A total of 8195-minutes clear-sky samples and 69318-minutes cloudy-sky samples are used in the analysis.

Fig. 1 shows how our method determines clear-sky conditions. DSR_{obs} presents a smooth temporal variation from sunrise to about 14:00, August 19, 2016 (LST), being consistent with DSR_{clr}. Similarly, DLR also varies very smoothly during this period and standard deviations of 21-min DLRs are generally less than 5 W m^{-2}. Both facts suggest that the sky is sunny and cloudless. This inference is supported by MPL backscatter measurements that do not detect any clouds overhead. Contrarily, an abruptly changes of 1-min DSR_{obs} and DLR are evident and we can see DSR_{obs} occasionally exceeds the expected DSR_{clr}, indicating occurrence of thin or fair weather cumuli clouds. MPL detect a persistent cloud layer at 3 km above ground during 14:00-17:00 LST, which agrees with DSR and DLR measurements very well. Two-layer clouds are observed by MPL until to sunset, which is accompanied by highly variation of observed DSR and DLR.

3.2 Cloud fraction estimation

Given synoptic cloud observations are very limited and temporally sparse, various parameterizations using DSR or DLR data have been developed to estimate the cloud fraction (CF) or called cloud modulate factor (CMF) (e.g., Deardorff, 1978; Marty and Philipona, 2000; Durr and Philipona, 2004; Long et al., 2006; 2008). Because of the good agreement between clear-sky DSR_{obs} and DSR_{cal} calculated by the Iqbal C calculations (Iqbal, 1983), with mean bias of 1.7 Wm^{-2} and root mean square error (RMSE) of 10.7 Wm^{-2}, we use Deardorff 's method to calculate CF from DSR_{obs} and DSR_{cal}. The method is based on a fairly simple cloud modification to DSR as follows.

$$CF = 1 - \frac{DSR_{obs}}{DSR_{cal}} \quad (1)$$

To avoid the error caused by abrupt DSR variation, 21-min DSR samples rather than its instantaneous measurements are used to calculate CF here.

4 Results

4.1 Clear-sky DLR parameterization evaluation and localization

Eleven clear-sky DLR (DLR_{clr}) parameterizations (Table 2) are evaluated based

Atmos. Chem. Phys. Discuss., https://doi.org/10.5194/acp-2019-397
Manuscript under review for journal Atmos. Chem. Phys.
Discussion started: 6 May 2019

on 1-min DLR measurements under unambiguously cloud-free conditions. To compare the performance of these 11 models, RMSE and the coefficient of determination (R^2) are shown by a Taylor diagram in Fig. 2(a). The Brutsaert (1975); Konzelmann (1994); Dilley and O'Brien (1998) and Prata (1995) models show relatively smaller RMSE (generally < 15 $W \cdot m^{-2}$) and larger R^2 (>0.95). One possible reason is that those parameterizations were developed in cool and dry areas (like England in Brutsaert (1975), Greenland in Konzelmann (1994) and Australian desert in Prata (1995). The climate in those areas is likely similar to that in TP, so one would expect the coefficients in those parameterizations are also suitable in TP. The higher RMSE (>37 W m^{-2}) and the lower R^2 (~0.7) for Swinbank (1963) and Idso and Jackson (1969). Both used T as the sole parameter. The essential point was that the screen temperature is a better indicator of the mass of radiatively active water vapor than the surface vapor pressure. However, previous studies have suggested that these methods would produce substantially large RMSE (>37.5 $W \cdot m^{-2}$) and low R^2 (<0.75) (Duarte et al., 2006). The reason is that the atmospheric effective emissivity is more sensitive to the water vapor profile than the mass of radiatively active water vapor when the surface layer is dry compared to the whole column (Dupon et al., 2008). Furthermore, DLR_{clr} is more much sensitive to variation of water vapor content over the TP than humid environment. Careful consideration of water vapor effect on DLR is obviously required over the TP.

The coefficients in eleven parameterizations (Table 2) were originally calibrated and determined in different geographical locations; therefore, they may not be the optimal values for the usage in the TP. Thus we take use of 1-min clear-sky DLR samples to locally calibrate the parameters of these parametrizations. We used k-fold cross-validation method to determine the local parameters. This method has two main advantages：i）less error rate because it repeatedly fits the statistical learning method using training data sets,. ii）decreasing the error rate by using random training/validation data sets for multiple times (James et al., 2013). Here, all data was randomly divided into 10 groups of approximately equal size, the coefficients are computed by using 9 groups as training set, and the remained one as validation. This

Atmos. Chem. Phys. Discuss., https://doi.org/10.5194/acp-2019-397
Manuscript under review for journal Atmos. Chem. Phys.
Discussion started: 6 May 2019

Atmospheric Chemistry and Physics
Open Access
Discussions

procedure is repeated 10 times to get the representational value (with the lowest test error) of coefficients in different parameterizations.

The non-linear least-squares fitting of the DLR_{clr} parameterizations (Table 2) resulted in the coefficient values in Table 3. For each fitted parameterization, we calculated RMSE and R^2 and the results are shown in Fig. 2(b). When using the parameterizations with the locally fitted parameters (Fig. 2(b)), the accuracy of the parameterization relative to the published values is substantially improved. Most RMSEs are less than 10 $W \cdot m^{-2}$ except the parameterization proposed by Swinbank (1963) and Idso and Jackson (1969) that still produced the worst results (with R^2 of 0.71 and RMSE of 15 $W \cdot m^{-2}$) even the parameters are locally calibrated. The Dilley and O'Brien's parameterization, which was initially developed by considering the adaptation of climatological diversities, is expected to be able to fit the measurements in tropical, mid-latitude and Polar Regions. This expectation is verified by its wide deployment in DLR_{clr} estimations in different climate regimes and altitude levels, for example, in the tropical lowland (eastern Pará state, Brazil) and the mild mountain area (Boulder, the United States) (Marthews et al., 2012; Li et al., 2017). The present study also confirmed that Dilley and O'Brien is the best clear-sky parameterization over the TP. This parameterization was also proved to be the most reliable estimates of DLR_{clr} in the TP (Zhu et al., 2017). The locally calibrated equation is as follows.

$$\mathrm{DLR}_{clr} = -2.53 + 158.10 \times \left(\frac{T}{273.16}\right)^6 + 106.40 \times \left(\frac{46.50 \times \frac{e}{T}}{2.50}\right)^{\frac{1}{2}} \quad (2)$$

The RMSE and R^2 of Eq.(2) are ~3.8 $W \cdot m^{-2}$ and > 0.98 respectively, which are substantially lower than those in previous studies in the TP, for example, the RMSE was 9.5 $W \cdot m^{-2}$ in Zhu et al. (2017). Note that the parameters here differ quite a lot from those in the reference (Zhu et al., 2017) that is shown in Eq. (3).

$$\mathrm{DLR}_{clr} = 30.00 + 157.00 \times \left(\frac{T}{273.16}\right)^6 + 97.93 \times \left(\frac{46.50 \times \frac{e}{T}}{2.50}\right)^{\frac{1}{2}} \quad (3)$$

Fig.3 shows the comparison of instantaneous clear-sky DLR measurements as a function of calculations by Eq. (2) and by Eq. (3). It is seen that measurements are in good agreement with calculations of Eq. (2), as shown by an overwhelmingly large number of data points falling along or overlap the 1:1 line. By contrast, clear-sky

DLR is always overestimated by Eq. (3). Note that Eq. (3) was derived from 1-hour DLR measurements, which was discriminated to be taken under clear-sky or cloudy conditions based on human observation at even lower resolution (every 3-6 hours). Both factors are likely to introduce potential cloud contamination on clear-sky discrimination due to rapid variations of cloud. The presence of clouds would lead to a larger DLR value relative to that in clear sky, which is most likely cause for the overestimation of Eq. (3). Significant impacts on the monthly and yearly radiation budget of the same magnitude are not avoided as a result of persisting overestimation of DLR by Eq. (3).

4.2 Parameterization of cloudy-sky DLR

The parameterizations of cloudy-sky DLR (DLR_{cld}) are based on estimated DLR_{clr} coupled with the effect of cloudiness or cloud emissivity, which depends primarily on CF, and some other cloud parameters, like CBH and cloud type (Arking, 1990; Viúdez-Mora et al., 2014). Four parameterizations (Table 4), which modifies the bulk emissivity depending on CF, are assessed and locally calibrated in this section.

DLR_{clr} is estimated according to Eq. (2) with the locally fitted coefficients. The fitted values of the coefficients (using k-Fold Cross-Validation) of the four parameterizations are presented in Table 5, and the RMSE and R^2 of original and locally fitted parameterizations in TP are presented in Fig. 4.

Relative to that under clear-sky conditions, cloudy parameterizations using the given parameters produced larger RMSE (generally exceeding 35 $W{\cdot}m^{-2}$) except that developed by Jacobs (1978) (RMSE of 18 $W{\cdot}m^{-2}$). R^2 was generally smaller than 0.9. RMSE decreased significantly in Maykut and Church (1973) and Sugita and Brutsaert (1993) as locally calibrated parameters were used. Relative smaller and almost no RMSE improvements were found for the methods developed by Konzelmann (1994) and Jacobs (1978).

Eq. (4) shows the best cloudy-sky parameterization over TP by combining the clear-sky parameterization of Dilley and O'Brien (1998) with the cloud modulation correction scheme of Jacobs (1978).

$$DLR_{cld} = (1 + 0.23 \times CF) \times (59.38 + 113.70 \times \left(\frac{T}{273.16}\right)^6 + 96.96 \times \left(\frac{46.50 \times \frac{e}{T}}{2.50}\right)^{\frac{1}{2}}) \quad (4)$$

The RMSE and R^2 are ~18 W·m^{-2} and ~0.89. RMSE here is close to 15 W m^{-2} obtained at different altitudes in Swiss (Gubler et al., 2012), and slightly lower than 23 W m^{-2} in mountain area in Germany (Iziomon et al., 2003). Comparing to previous studies over the TP (RMSE of 22 W m^{-2} in Zhu et al., 2017), our cloudy model also produces better results.

4.3 Effect of CBH on DLR under Overcast Conditions

Since clouds behave approximately as a blackbody, the most relevant cloud parameter (besides CF) to DLR under overcast skies (DLR_{ovc}) is the temperature of its lower boundary (CBH). Radiative transfer model simulation has suggested that CBH under overcast conditions is an important modulator for the DLR. The cloud radiation effect (CRE), the difference between DLR_{obs} and DLR_{clr}, decreases with increasing CBH at a rate of 4~12 W·m^{-2} that depends on climate profiles (Viúdez-Mora et al., 2014). This indicated that cloudy DLR parameterization can be improved if CBH effect is considered.

The statistical relationship between CRE and CBH under overcast conditions in the TP is presented in Fig. 5, a box plot of CBH versus CRE. The peak and median values of CRE decrease with the increase of CBH. With the increase of CBH, the variation range of the CRE rises, ranging from 25 to 50 W·m^{-2}, as a result of the specific meteorological and cloud conditions. Compared to that at Girona, Spain, a low altitude mid-latitude site (Viúdez-Mora, et al., 2014), CRE in the TP is generally lower by 5~10 W·m^{-2}. This is likely associated with the fact that clouds in the TP with the same CBH as that in Girona have relatively lower temperature, thereby producing lower radiative effect on DLR. It is interesting that the decreasing tendency of CRE with CBH is apparent. CRE is about 70 W·m^{-2} for clouds < 1 km and decreases to ~40 W·m^{-2} for clouds at 3~4 km in the TP. The decreasing rate of CRE with CBH is estimated to be -9.8 W·m^{-2}km^{-1} in the TP that is within the model simulations

Atmos. Chem. Phys. Discuss., https://doi.org/10.5194/acp-2019-397
Manuscript under review for journal Atmos. Chem. Phys.
Discussion started: 6 May 2019

Atmospheric Chemistry and Physics Discussions

(Viúdez-Mora et al. 2014).

To consider CBH effect under overcast conditions, we introduced a modified parameterization similar as that in Viúdez-Mora et al. (2014).

$$DLR_{ovc} = 1.23 \times DLR_{clr} \times (1.01 - 0.06 \times \mathrm{CBH}) \qquad (5)$$

The bias and RMSE of Eq.(5) between measurements and calculations is 1.3 W·m^{-2} and 16.5 W·m^{-2}, respectively, which are significantly lower than that of Eq.(4) (10.3 W m^{-2} and 21.4 W m^{-2}) in overcast conditions. This result indicates a remarkable improvement in the estimation of DLR under overcast conditions by introducing CBH to the DLR parameterization.

5 Discussion and conclusions

The parameterization of clear-sky DLR requires a well-defined distinction between clear-sky and cloudy-sky situations that commonly depends on human cloud observations 4~6 times each day. Human observations are subjective in nature and have a very limited temporal resolution that obviously cannot capture dramatic variations of clouds. Furthermore, synoptic（human cloud observations show the tendency to stronger weight the horizon that DLR is not highly sensitive (Marty and Philipona). Therefore, parameterization of clear-sky DLR based on synoptic sky observations is hence very likely biased as a consequence of improper selection of clear-sky measurements. This issue should be considered cautiously because it is essential to precisely quantify aerosol and cloud radiative effects that rely on precise identification of cloud free references (Dupont et al., 2008b).

Using 1-min DSR and DLR at 3 stations over the TP, DLR parameterizations are evaluated and localized parameterizations have been developed. Potential CBH effect on overcast DLR is experimentally determined. Major conclusions are as follows.

Among 11 clear-sky DLR parameterizations tested in this study, these two methods using only atmospheric temperature largely deviated from other parameterizations. DLR estimation can be improved by localization of these parameterizations. The best method suitable for the TP is the parameterization developed by Dilley and O'Brien (1997). The locally calibrated Dilley and O'Brien model can produce clear-sky DLR with a RMSE of 3.8 W·m^{-2}.

Overcast DLR is highly sensitive to CBH. The parameterization in this case can be substantially improved by consideration of CBH effect. The bias between model calculations and measurements decreases from 10.3 W m^{-2} to 1.3 W m^{-2} when CBH effect is introduced

A broadly representative of existing DLR parameterizations with good performance was assessed over the TP, while this did not imply that our sample of techniques was either exhaustive or optimal in all applications. We only focused on daytime DLR parameterization in TP since DSR is used in the cloud-screening method. Given a significant role of DLR played in the surface energy budget during nighttime, it is highly desirable to perform further study on the nighttime DLR parametrization in future. These results are based on summer DLR measurements in TP, so the conclusions here need to be tested in other seasons, especially in winter when DLR has been observed to increase in the TP (Rangwala et al., 2009). These further study would shed new light on how DLR is related to temperature and water vapor and why DLR has changed in the TP.

Author contributions. XD and XA designed the experiments and MQ carried them out. MQ and JQ prepared the manuscript with contributions from all co-authors.

Competing interests. The authors declare that they have no conflict of interest.

Data availability. The data can be obtained from the corresponding author upon request.

Acknowledgements: This work was supported by the Strategic Priority Research Program of Chinese Academy of Sciences (XDA17010101), the National Key R&D Program of China (2017YFA0603504), the National Natural Science Foundation of China (91537213 and 91637107), the Special Fund for Meteorological Research in the Public Interest (GYHY201106023), and the Science and Technological Innovation Team Project of Chinese Academy of Meteorological Science (2013Z005). We greatly appreciate Dr. Q. He for providing the MPL Lidar measurement images and derived CBH data.

Atmos. Chem. Phys. Discuss., https://doi.org/10.5194/acp-2019-397
Manuscript under review for journal Atmos. Chem. Phys.
Discussion started: 6 May 2019

References

Ångström, A.: A study of the radiation of the atmosphere, Smithsonian Miscellaneous Collection, 65, 1–159, 1915.

Arking, A.: The radiative effects of clouds and their impact on climate, Bull. Am. Meteorol. Soc., 72, 795-813, 10.1175/1520-0477(1991)072<0795:Treoca>2.0.Co;2, 1991.

Brunt, D.: Notes on radiation in the atmosphere, Q. J. Roy. Meteorol. Soc., 58, 389–420, 1932.

Brutsaert, W.: On a derivable formula for long-wave radiation from clear skies, Water Resour. Res., 11, 742–744, 1975.

Carmona, F., Rivas, R., and Caselles, V.: Estimation of daytime downward longwave radiation under clear and cloudy skies conditions over a sub-humid region, Theor. Appl. Climatol., 115, 281-295, 10.1007/s00704-013-0891-3, 2014.

Che, H. Z., Zhao, H. J., Wu, Y. F., Xia, X. G., Zhu, J., Wang, H., Wang, Y. Q., Sun, J. Y., Yu, J., Zhang, X. Y., and Shi, G. Y.: Analyses of aerosol optical properties and direct radiative forcing over urban and industrial regions in Northeast China, Meteorol. Atmos. Phys., 127, 345-354, 10.1007/s00703-015-0367-3, 2015.

Crawford, T. M., and Duchon, C. E.: An improved parameterization for estimating effective atmospheric emissivity for use in calculating daytime downwelling longwave radiation, J. Appl. Meteorol., 38, 474–480, 1998.

Deardorff, J. W.: Efficient prediction of ground surface temperature and moisture, with an inclusion of a layer of vegetation. J. Geophys. Res., 83, 1889–1903, 1978.

Dilley, A. C., and O'Brien, D. M.: Estimating downward clear sky long-wave irradiance at the surface from screen temperature and precipitable water, Q. J. Roy. Meteorol. Soc., 124a, 1391–1401, 1997.

Dozier, J., and Frew, J.: Rapid calculation of terrain parameters for radiation modeling from digital elevation data, IEEE T. Geosci. Remote, 28, 963–969, 1990.

Duan, A., and Wu, G.: Change of cloud amount and the climate warming on the Tibetan Plateau, Geophys. Res. Lett., 33, 10.1029/2006gl027946, 2006.

Duarte, H. F., Dias, N. L., and Maggiotto, S. R.: Assessing daytime downward longwave radiation estimates for clear and cloudy skies in Southern Brazil, Agr. Forest. Meteorol., 139, 171-181, 10.1016/j.agrformet.2006.06.008, 2006.

Duchon, C. E., and O'Malley, M. S.: Estimating cloud type from pyranometer observations, J. Appl. Meteorol., 38, 132-141, 1999.

Dupont, J. C., Haeffelin, M., Drobinski, P., and Besnard, T.: Parametric model to estimate clear-sky longwave irradiance at the surface on the basis of vertical distribution of humidity and temperature, J. Geophys. Res., 113, 10.1029/2007jd009046, 2008a.

Dupont, J. C., Haeffelin, M., and Long, C.N.: Evaluation of cloudless-sky periods detected by shortwave and longwave algorithms using lidar measurements, Geophys. Res. Lett., 35, L10815, doi:10.1029/2008GL033658, 2008b.

Durr, B., and Philipona, R.: Automatic cloud amount detection by surface longwave downward radiation measurements, J. Geophys. Res., 109, 9, 10.1029/2003jd004182, 2004.

Gubler, S., Gruber, S., and Purves, R. S.: Uncertainties of parameterized surface downward clear-sky shortwave and all-sky longwave radiation, Atmos. Chem. Phys., 12, 5077-5098, 10.5194/acp-12-5077-2012, 2012.

He, Q. S., Li, C. C., Ma, J. Z., Wang, H. Q., Shi, G. M., Liang, Z. R., Luan, Q., Geng, F. H., and Zhou, X. W.: The properties and formation of cirrus clouds over the Tibetan Plateau based on summertime lidar measurements, J. Atmos. Sci., 70, 901-915, 10.1175/jas-d-12-0171.1, 2013.

Idso, S. B.: A set of equations for full spectrum and 8 to 14 μm and 10.5 to 12.5 μm thermal radiation from cloudless skies, Water Resour. Res., 17, 295–304, 1981.

Iqbal, M.: An Introduction to Solar Radiation, Academic Press, Toronto, Canada, 1983.

Iziomon, M. G., Mayer, H., and Matzarakis, A.: Downward atmospheric longwave irradiance under clear and cloudy skies: measurement and parameterization, J. Atmos. Solar-Terr. Phys., 65, 1107–1116, 2003.

Jacobs, J.D.: Radiation climate of Broughton Island, in: Energy Budget Studies in Relation to Fast-ice Breakup Processes in Davis Strait, edited by Barry, R. G. and Jacobs, J. D., Inst. of Arctic and Alp. Res. Occas. Paper No. 26. University of Colorado, Boulder, pp. 105–120, 1978.

James, G., Witten, D., Hastie, T., and Tibshirani, R.: An Introduction to Statistical Learning: with Applications in R, Springer-Verlag New York, USA, 2013.

Kiehl, J. T., and Trenberth, K. E.: Earth's annual global mean energy budget. Bull. Am. Meteorol. Soc., 78, 197-208, 1997.

Atmos. Chem. Phys. Discuss., https://doi.org/10.5194/acp-2019-397
Manuscript under review for journal Atmos. Chem. Phys.
Discussion started: 6 May 2019

Atmospheric Chemistry and Physics Discussions

Konzelmann, T., van de Wal, R. S. W., Greuell, W., Bintanja, R., Henneken, E. A. C., and Abe-Ouchi, A.: Parameterization of global and longwave incoming radiation for the Greenland Ice Sheet, Global. Planet. Change., 9, 143–164, 1994.

Kruk, N. S., Vendrame, I. F., da Rocha, H. R., Chou, S. C., and Cabral, O.: Downward longwave radiation estimates for clear and all-sky conditions in the Sertozinho region of So Paulo, Brazil, Theor. Appl. Climatol., 99, 115-123, 2010.

Li, M. Y., Jiang, Y. J., and Coimbra, C. F. M.: On the determination of atmospheric longwave irradiance under all-sky conditions, Sol. Energy., 144, 40-48, 10.1016/j.solener.2017.01.006, 2017.

Liang, H., Zhang, R. H., Liu, J. M., Sun, Z. A., and Cheng, X. H.: Estimation of hourly solar radiation at the surface under cloudless conditions on the Tibetan Plateau using a simple radiation model, Adv. Atmos. Sci., 29, 675-689, 10.1007/s00376-012-1157-1, 2012.

Long, C. N., Ackerman, T. P., Gaustad, K. L., and Cole, J. N. S.: Estimation of fractional sky cover from broadband shortwave radiometer measurements, J. Geophys. Res., 111, 11, 10.1029/2005jd006475, 2006.

Long, C. N., and Turner, D. D.: A method for continuous estimation of clear-sky downwelling longwave radiative flux developed using ARM surface measurements, J. Geophys. Res., 113, 16, 10.1029/2008jd009936, 2008.

Marthews, T. R., Malhi, Y., and Iwata, H.: Calculating downward longwave radiation under clear and cloudy conditions over a tropical lowland forest site: an evaluation of model schemes for hourly data, Theor. Appl. Climatol., 107, 461-477, 10.1007/s00704-011-0486-9, 2012.

Marty, C., and Philipona, R.: The Clear-Sky Index to separate clear-sky from cloudy-sky situations in climate research, Geophys. Res. Lett., 27, 2649-2652, 10.1029/2000gl011743, 2000.

Maykut, G. A., and Church P. E.: Radiation climate of Barrow, Alaska, 1962–1966, J. Appl. Meteorol., 12, 620–628, 1973.

Meloni D, Biagio C D, Sarra A D, et al.: Accounting for the Solar Radiation Influence on Downward Longwave Irradiance Measurements by Pyrgeometers, J. Atmos. Ocean. Tech., 29,1629-1643, 2012.

Niemelä, S., Räisänen, P., and Savijärvi, H.: Comparison of surface radiative flux parameterizations: Part I: Longwave radiation, Atmos. Res., 58, 1–18, 2001a.

Orsini, A., Tomasi, C., Calzolari, F., Nardino, M., Cacciari, A., and Georgiadis, T.:

Atmos. Chem. Phys. Discuss., https://doi.org/10.5194/acp-2019-397
Manuscript under review for journal Atmos. Chem. Phys.
Discussion started: 6 May 2019

Cloud cover classification through simultaneous ground-based measurements of solar and infrared radiation, Atmos. Res., 61, 251-275, 10.1016/s0169-8095(02)00003-0, 2002.

Prata, A. J.: A new long-wave formula for estimating downward clear-sky radiation at the surface, Q. J. Roy. Meteorol. Soc., 122, 1127–1151, 1996.

Rangwala, I., Miller, J. R., and Xu, M.: Warming in the Tibetan plateau: possible influences of the changes in surface water vapor. Geophys. Res. Lett., 36, 295-311, 2009.

Satterlund, D. R.: An improved equation for estimating longwave radiation from the atmosphere, Water Resour. Res., 15, 1649–1650, 1979.

Stephens, G. L., Wild, M., Stackhouse, P. W., Jr., L'Ecuyer, T., Kato, S., and Henderson, D. S.: The global character of the flux of downward longwave radiation, J. Climate., 25, 2329-2340, 10.1175/jcli-d-11-00262.1, 2012.

Stoffel, T.: Solar infrared radiation station (SIRS) handbook, Tech. Rep., ARM TR-025, Atmos. Radiat. Measure. Program, U.S. Dep. of Energy, Washington, D.C, 2005.

Sugita, M., and Brutsaert, W.: Cloud effect in the estimation of instantaneous downward longwave radiation, Water Resour. Res., 29, 599-605, 10.1029/92wr02352, 1993.

Swinbank, W. C.: Long-wave radiation from clear skies, Q. J. Roy. Meterol. Soc., 89, 330–348, 1963.

Viúdez-Mora, A., Costa-Surós, M., Calbó, J., and González, J. A.: Modeling atmospheric longwave radiation at the surface during overcast skies: The role of cloud base height, J. Geophys. Res. Atmos., 120, 199–214, doi:10.1002/ 2014JD022310, 2014.

Wang, K., and Liang, S.: Global atmospheric downward longwave radiation over land surface under all-sky conditions from 1973 to 2008, J. Geophys. Res., 114, 10.1029/2009jd011800, 2009.

Wang, K., and Dickinson, R. E.: Global atmospheric downward longwave radiation at the surface from ground-based observations, satellite retrievals, and reanalyses, Reviews of Geophysics, 51, 150-185, 10.1002/rog.20009, 2013.

Wu, G., Liu, Y., Wang, T., Wan, R., Liu, X., Li, W., Wang, Z., Zhang, Q., Duan, A. and Liang, X.: The influence of mechanical and thermal forcing by the Tibetan Plateau on Asian climate, J. Hydro., 8, 770-789, 2007.

Atmos. Chem. Phys. Discuss., https://doi.org/10.5194/acp-2019-397
Manuscript under review for journal Atmos. Chem. Phys.
Discussion started: 6 May 2019

Atmospheric Chemistry and Physics Discussions

Yang, K., Ding, B., Qin, J., Tang, W., Lu, N., and Lin, C.: Can aerosol loading explain the solar dimming over the Tibetan Plateau?, Geophys. Res. Lett., 39, 10.1029/2012gl053733, 2012.

Zhu, M. L., Yao, T. D., Yang, W., Xu, B. Q., and Wang, X. J.: Evaluation of parameterizations of incoming longwave radiation in the high-mountain region of the Tibetan Plateau, J. Appl. Meteorol. Climatol., 56, 833-848, 10.1175/jamc-d-16-0189.1, 2017.

Table 1: Description of station and measurement (magnitude and variability) in the Tibetan Plateau

Site	Altitude (m)	Period	T (°C)	*e* (hPa)	DLR ($W \cdot m^{-2}$)	Data Points
NQ	4507	2011.7.20-2011.8.26	9.4±8	7.4±5	242.75±40	52980
NC	2290	2014.6.7-2014.7.31	16.8±10	13.4±4	368.25±40	69609
AL	4279	2016.5.27-2016.9.22	7.8±4	4.8±4	253.11±50	86596

Atmos. Chem. Phys. Discuss., https://doi.org/10.5194/acp-2019-397
Manuscript under review for journal Atmos. Chem. Phys.
Discussion started: 6 May 2019

Atmospheric Chemistry and Physics
Open Access
Discussions

Table 2. 11 clear-sky DLR parameterizations and associated specific conditions

Reference	Clear-Sky Parameterization	Conditions
Angstrom (1915)	$DLR_{clr} = \{0.83 - 0.18 \times 10^{-0.067e})\}\sigma T^4$	Alt.: 1650, 3500m a.s.l T: 10~30°C *e*: 4~17hPa
Brunt (1932)	$DLR_{clr} = (0.52 + 0.065\sqrt{e})\sigma T^4$	Alt.: 6, 1650, 3500m a.s.l T: -4~30°C *e*: 2.5~16hPa
Swinbank (1963)	$DLR_{clr} = 5.31 \times 10^{-13} T^6$	Alt: 2m a.s.l T: 8~29°C *e*: 8~30hPa
Idso and Jackson (1969)	$DLR_{clr} = (1 - 0.261 \cdot \exp(-0.000777 \times (273 - \mathrm{T})^2))\sigma T^4$	Alt.: 3, 331m a.s.l T: -45~45°C
Brutsaert (1975)	$DLR_{clr} = 1.24 \left(\frac{e}{T}\right)^{\frac{1}{7}} \sigma T^4$	Alt.: 6, 1650, 3500m a.s.l T: -4~30°C *e*: 2.5~-16hPa
Satterlund (1979)	$DLR_{clr} = 1.08\left(1 - \exp\left(-e^{\frac{T}{2016}}\right)\right)\sigma T^4$	Alt.: 594m a.s.l T: -37~36°C *e*: 0~18hPa
Idso (1981)	$DLR_{clr} = \left(0.7 + 5.95 \times 10^{-5} \times e \times \exp\left(\frac{1500}{\mathrm{T}}\right)\right)\sigma T^4$	Alt.: 331m a.s.l T: -15~5°C *e*: 2~6hPa
Konzelmann (1994)	$DLR_{clr} = \left(0.23 + 0.443\left(\frac{e}{T}\right)^{\frac{1}{8}}\right)\sigma T^4$	Alt.: 340~3230m a.s.l T: -16~6°C *e*: 1.5~5.5hPa
Prata (1995)	$DLR_{clr}=(1-(1+46.5\frac{e}{T}) \times \exp(-(1.2+3\times 46.5\frac{e}{T})^{0.5}))\,\sigma T^4$	Not specified
Dilley and O'Brien (1998)	$DLR_{clr}=59.38+113.7\left(\frac{T}{273.16}\right)^6 + 96.96\sqrt{46.5\frac{e}{T}/2.5}$	Not specified
Iziomon (2001)	$DLR_{clr} = \left(1 - 0.43\exp\left(-\frac{11.5e}{T}\right)\right)\sigma T^4$	Alt.: 1489m a.s.l $\bar{T}$=4.4°C $\bar{e}$ =7.4hPa

*Where e is screen-level water vapor pressure in hPa and T represents surface temperature in K

Atmospheric Chemistry and Physics Discussions
Open Access
EGU

Table 3. Locally fitted clear-sky DLR parameterizations in TP

Reference	Locally fitted Clear-Sky Parameterization
Angstrom(1915)	$\mathrm{DLR}_{clr} = \{0.8 - 0.19 \times 10^{-0.068e}\}\sigma T^4$
Brunt(1932)	$\mathrm{DLR}_{clr} = (0.56 + 0.07\sqrt{e})\sigma T^4$
Swinbank(1963)	$\mathrm{DLR}_{clr} = 4.7 \times 10^{-13} T^6$
Idso & Jackson(1969)	$\mathrm{DLR}_{clr} = (1 - 0.36 \cdot \exp(-0.00065 \times (273 - \mathrm{T})^2))\sigma T^4$
Brutsaert(1975)	$\mathrm{DLR}_{clr} = 1.03 \left(\frac{e}{T}\right)^{0.09} \sigma T^4$
Satterlun (1979)	$\mathrm{DLR}_{clr} = \left(1 - \exp\left(-e^{\frac{T}{2016}}\right)\right)\sigma T^4$
Idso(1981)	$\mathrm{DLR}_{clr} = \left(0.63 + 7.5 \times 10^{-5} \times e \times \exp\left(\frac{1500}{\mathrm{T}}\right)\right)\sigma T^4$
Konzelmann(1994)	$\mathrm{DLR}_{clr} = \left(0.23 + 0.45\left(\frac{e}{T}\right)^{0.13}\right)\sigma T^4$
Prata(1995)	$\mathrm{DLR}_{clr}=(1-(1+46.5\frac{e}{T})\ \times\exp(-(1+3\times46.5\frac{e}{T})^{0.5}))\ \sigma T^4$
Dilley and O'Brien(1998)	$\mathrm{DLR}_{clr}=-2.54+158.1\left(\frac{T}{273.16}\right)^6 + 106.4\sqrt{46.5\frac{e}{T}/2.5}$
Iziomon(2001)	$\mathrm{DLR}_{clr} = \left(1 - 0.38\exp\left(-\frac{14.52e}{T}\right)\right)\sigma T^4$

Table 4. 4 Cloudy-sky DLR Parameterizations in the references

Reference	Cloudy-Sky Parameterization
Maykut and Church, 1973	$DLR_{cld} = (0.7855 + 0.000312CF^{2.75})\sigma T^4$
Jacobs, 1978	$DLR_{cld} = (1 + 0.26CF)DLR_{clr}$
Sugita and Brutsaert, 1993	$DLR_{cld} = (1 + 0.0496CF^{2.45})\ DLR_{clr}$
Konzelmann, 1994	$DLR_{cld} = (1 - CF^4)DLR_{clr} + 0.954CF^4\sigma T^4$

Atmos. Chem. Phys. Discuss., https://doi.org/10.5194/acp-2019-397
Manuscript under review for journal Atmos. Chem. Phys.
Discussion started: 6 May 2019

Atmospheric Chemistry and Physics
Discussions

Table 5. Locally fitted cloudy-sky DLR parameterizations in TP

Reference	Locally fitted Cloudy-Sky Parameterization
Maykut and Church, 1973	$DLR_{cld} = (0.85 + 0.01CF^3)\sigma T^4$
Jacobs, 1978	$DLR_{cld} = (1 + 0.23CF)DLR_{clr}$
Sugita and Brutsaert,1993	$DLR_{cld} = (1 + 0.2CF^{1.3})\ DLR_{clr}$
Konzelmann, 1994	$DLR_{cld} = (1 - CF^{3.5})DLR_{clr} + CF^{3.5}\sigma T^4$

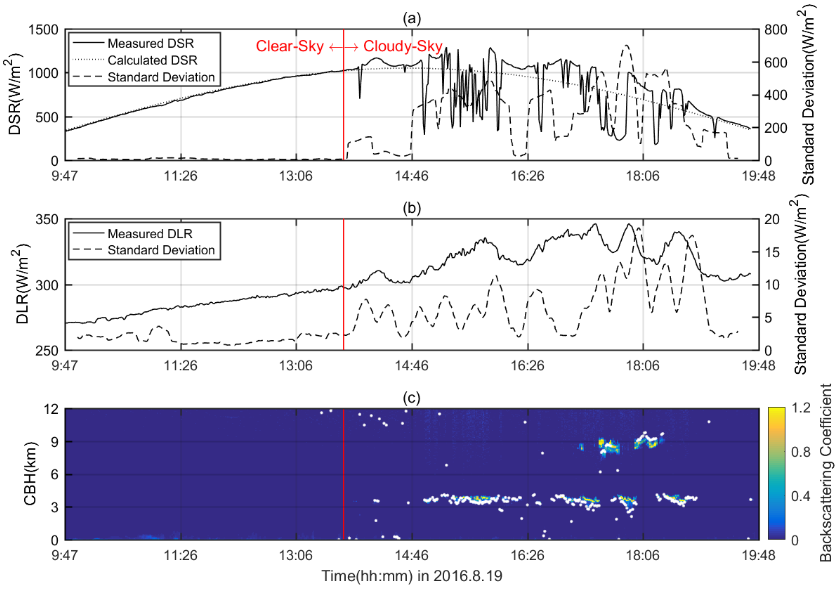

Fig. 1. Time series of one-day sample on 2016.8.19 transited from clear-skies to cloudy-skies: (a) measured (black line) and calculated (dotted black line) downward shortwave radiation and its 21-min standard deviation (grey line), (b) measured downward longwave radiation and 21-min standard deviation and (c) MPL backscattering coefficient (color bar) and the cloud base height (white dots).

Atmos. Chem. Phys. Discuss., https://doi.org/10.5194/acp-2019-397
Manuscript under review for journal Atmos. Chem. Phys.
Discussion started: 6 May 2019

Atmospheric Chemistry and Physics
Open Access
Discussions

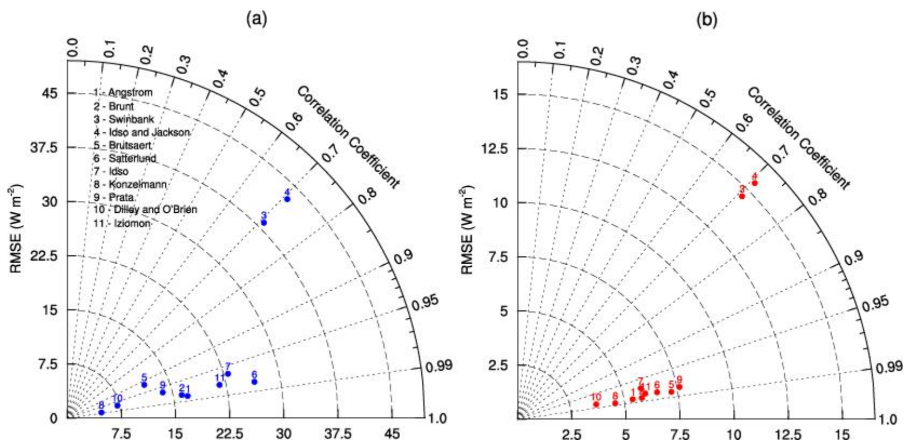

Fig. 2. RMSE and R^2 for the clear-sky DLR parameterizations using original (a) and locally calibrated (b) coefficient values.

Atmos. Chem. Phys. Discuss., https://doi.org/10.5194/acp-2019-397
Manuscript under review for journal Atmos. Chem. Phys.
Discussion started: 6 May 2019

615

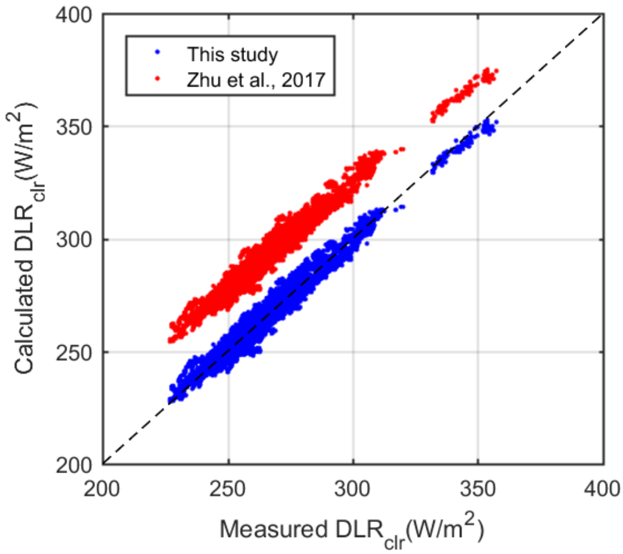

616

617 Fig. 3. Scatter plots of instantaneous clear-sky DLR data from measurements as a
618 function of calculations by this study (blue dots) and by Zhu et al. (2017) (red
619 dots).The dash black line is the 1:1 line.

620

Atmos. Chem. Phys. Discuss., https://doi.org/10.5194/acp-2019-397
Manuscript under review for journal Atmos. Chem. Phys.
Discussion started: 6 May 2019

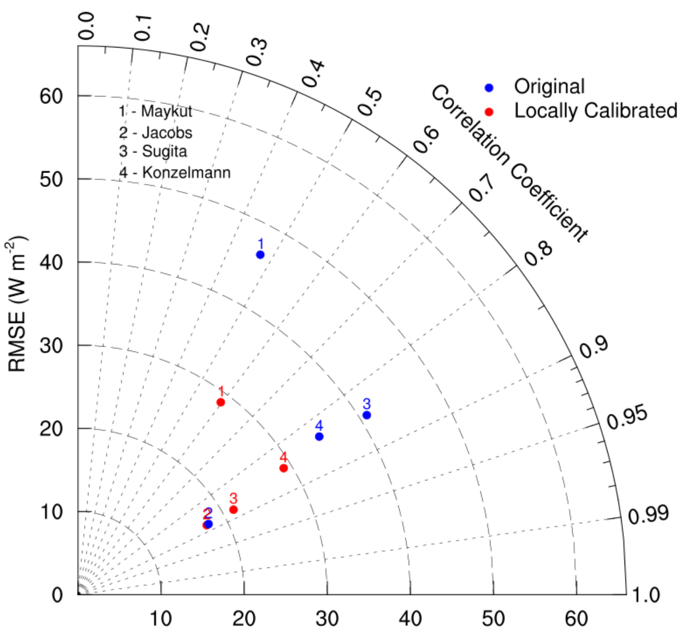

621
622 Fig. 4. RMSE and R^2 for the cloudy-sky DLR (DLR_{cld}) parameterizations using the
623 original (blue) and locally calibrated (red) coefficient values.
624
625

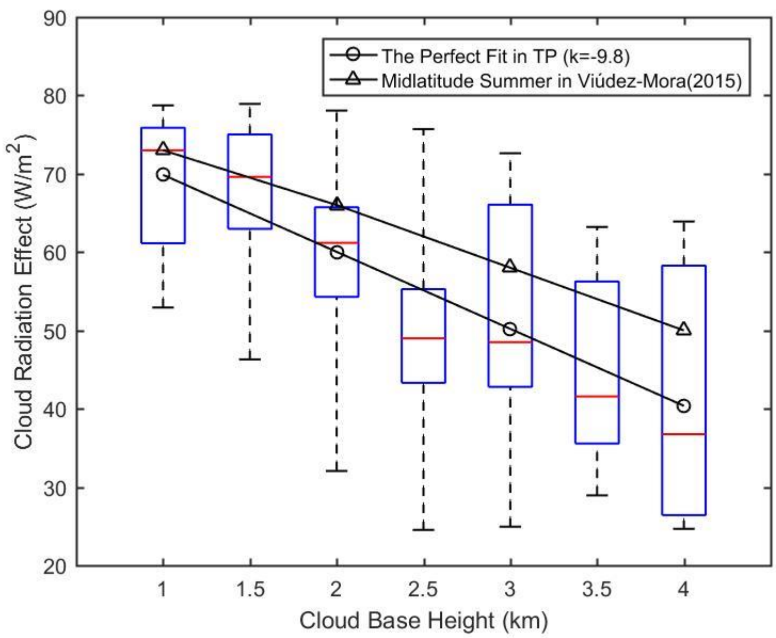

Fig. 5. Scatter plot of cloud radiative effect against MPL derived cloud base height are represented by box plot (the blue box indicates the 25th and 75th percentiles, the whiskers indicate 5th and 95th percentiles, the red middle line is the median). The black circles line and the black triangles is mean values of cloud radiative effect over TP in this study and in Girona, Spain (Viúdez-Mora et al., 2014).